Authors	Wenye Lin, Alan Green, Georgios Kokogiannakis and Paul Cooper
Title	Above-Roof Temperature Impacts on Heating Penalties of Large Cool Roofs in Australian Climates – Interim Report 1
ISBN	
Date	28/2/2019
Keywords	Cool roof, Dew, Condensation, Building energy performance, Sustainability
Publisher	
Preferred citation	

Australian Government
Department of Industry, Innovation and Science
Business Cooperative Research Centres Programme

Acknowledgements

The authors would like to acknowledge the contributions of Bluescope Steel, especially the ongoing involvement of Mark Eckermann and Jamie Adams in the project. We would also like to recognise contributions made to the previous stage of this project, which formed a basis for much of the work contained in this report, by our colleagues at the University of New South Wales: Riccardo Paolini, Shamila Haddad, Afroditi Synnefa, Mattheos Santamouris and Baojie Hek, and at the University of Wollongong: Laia Ledo Gomis, Ben Zeitsch, David Beecher, Zhenjun Ma and Buyung Kosasih.

This research was funded by the CRC for Low Carbon Living Ltd supported by the Cooperative Research Centres program, an Australian Government initiative.

Disclaimer

Any opinions expressed in this document are those of the authors. They do not purport to reflect the opinions or views of the CRCLCL or its partners, agents or employees.

The CRCLCL gives no warranty or assurance, and makes no representation as to the accuracy or reliability of any information or advice contained in this document, or that it is suitable for any intended use. The CRCLCL, its partners, agents and employees, disclaim any and all liability for any errors or omissions or in respect of anything or the consequences of anything done or omitted to be done in reliance upon the whole or any part of this document.

Peer Review Statement

The CRCLCL recognises the value of knowledge exchange and the importance of objective peer review. It is committed to encouraging and supporting its research teams in this regard.

The authors confirm that this document has been reviewed and approved by the project's program leader and steering committee. The program leader provided constructive feedback, which has been addressed.

Contents

Acknowledgements 2
Disclaimer 2
Peer Review Statement 2
Contents 3
List of Tables 4
List of Figures 5
Acronyms 6
Executive Summary 7
Introduction 8
Background 8
Aims 8
Method 8
Report outline 9
Literature Review 10
Previous work on roof condensation 10
Latent heat 10
Influence on radiative-optical properties 11
Condensation likelihood in the RP1037 dataset 13
Roof condensation model 14
Model development 14
Quasi-steady case studies 16
Above-roof temperature model 19
Applicability of the model to cold weather 19
Applicability of the model to other buildings 20
Revision of the above-roof temperature model 20
Conclusion 22

List of Tables

Table 1: Summary of parameters used for the comparison of the external heat transfer coefficients calculated using different models. 15

Table 2: Steady boundary conditions used in the modelling. 17

List of Figures

Figure 1: Comparison of outdoor air, dew point and spatially averaged roof surface temperatures, measured through a typical 24h period during the experiments. 13

Figure 2: Time in which the mean roof surface temperature, Ts, was below the local dew point temperature, Tdp, during experiments at a) Nowra, b) Shellharbour, and c) Wetherill Park. 13

Figure 3: Energy balance of a flat roof. 14

Figure 4: Comparison of external convective heat transfer coefficients calculated using different models, for a) Roof A, and b) Roof B. 14

Figure 5: Comparison of the apparent emissivity model with experimental data. 16

Figure 6: Effect of a water film on the apparent thermal emittance of roof surfaces. 16

Figure 7: Modelling results for Baseline case: a) for roof surface temperature, and b) for comparison of the roof surface temperatures considering different effects. 17

Figure 8: Effect of ambient humidity on the quasi-steady conditions reached after 4 simulated hours: a) temperatures and the condensation rate, and b) temperatures, given different condensation effects. 18

Figure 9: Effect of ambient air temperature on the quasi-steady conditions reached after 4 simulated hours: a) temperatures and the condensation rate, and b) heat fluxes. 18

Figure 10: Comparison of the range of conditions that occurred during the experiments in RP1037 (labelled 'Exp.'), with those from year-long building performance simulations of a shopping centre in seven Australian climate zones (labelled 'CZ1'–'CZ7'). 19

Figure 11: Histogram showing the occurrence of different wind speeds in reference meteorological year weather files for cities in climate zones 1–7. 20

Figure 12: Comparison of the thermal boundary layer shape parameter, α, obtained from experimental data with those predicted by the above-roof temperature model, in a) stable and b) unstable conditions. Experimental data has been represented by the mean (dot) and standard deviation (whiskers) of α within discrete bins. 21

Acronyms

BPS	Building performance simulation
CFD	Computational fluid dynamics
HVAC	Heating, ventilation and air-conditioning
PV	Photovoltaic
RMS	Root-mean squared
RMSE	Root-mean squared error
UDF	User-defined function

Executive Summary

This is the first interim report for project RP1037u1, an extension to the recently completed project RP1037 'Driving increased utilisation of cool roofs on large-footprint buildings'. Progress so-far in the project and preliminary findings have been summarised in this report.

The research has been focused on two key aspects of roof thermal performance that had, up until the time of writing, not been taken into account in most investigations into cool roof technology:

1. The condensation and evaporation of dew on the roof surface, and the effect this has on roof temperature by way of:
    a. The latent heat that is absorbed and released; and
    b. Any change in the effective radiative-optical properties of the roof top surface due to accumulated water.
2. The effect of roof temperature on above-roof air temperatures, and the influence this can have on the performance of rooftop heating, ventilation and air-conditioning (HVAC) equipment.

Research literature related to water condensation on roofs has been reviewed. The review demonstrated that the heat fluxes caused by the latent heat release and absorption and the changes in the radiative-optimal properties are the two key effects of dew on the roof thermal performance. The latent heat released/absorbed can be deduced from the convective heat transfer coefficient. However, most previous studies that were reviewed adopted convective heat transfer coefficient models that were arguably not appropriate for roof surfaces. In terms of the changes in the apparent roof surface emissivity, evidence has been presented that dew could significantly increase the thermal emittance of low-emittance surfaces. However, previous studies that were reviewed did not consider this effect.

Further analysis of the existing RP1037 experimental dataset has revealed that conditions often occurred (on ~80% of nights) that would allow dew to form on large roofs, and that roof surface temperatures can drop as much as 8°C below the dew-point temperature.

A roof condensation model has been developed, to quantify the effect that water condensation can have on roof temperatures. The influence of the ambient air temperature and humidity on the dew formation process has been explored in a set of quasi-steady cases. In the set of conditions investigated, condensation could cause a roof surface temperature deviation of 0.83°C, compared to a case in which condensation was not considered. During the remainder of RP1037u1, the roof condensation model will be applied to realistic, dynamic cases, to quantify the effects of dew on cool roof and low-emittance 'non-cool' roof performance.

The above-roof temperature model, developed in RP1037, has been further analysed in this report. The range of weather conditions and buildings for which it is valid have been quantified, and compared to the cases to which it was applied in RP1037. With regard to weather, all of the relevant variables (e.g. degree of cloud cover, solar heat flux, ambient temperature, etc.) influence the normalised above-roof temperature field via their effect on either: i) the wind speed, or ii) the temperature difference between the roof surface and 'ambient' air. The range of combinations of these two variables included in the RP1037 dataset coincides with those that arose in simulations in RP1037, except for at high wind speeds ($\gtrsim 10$ m s^{-1}). This does indicate that the degree of uncertainty surrounding outputs of the above-roof temperature model is relatively high at high wind speeds; however, such wind speeds were very infrequent in the cases of interest, and above-roof air temperatures have a diminished effect at high wind speeds, since enhanced convective heat transfer drives the roof surface temperature closer to the 'ambient' air temperature. Further validation of the above-roof temperature model would be valuable, but it can be concluded that the model is valid for the cases to which it was applied in RP1037.

A new, improved version of the above-roof temperature model has also been developed. It was found that by changing the mathematical form of the model for unstable conditions (i.e. when the roof surface is hotter than the 'ambient' air temperature), a superior fit to experimental data could be achieved. Thus, this new model should predict above-roof temperatures with more accuracy than the previous version, and will be suitable for use in conjunction with the roof condensation model developed here. The new above-roof temperature model has been outlined in this report.

Further work in RP1037u1 will apply the new roof condensation model and improved above-roof temperature model to a set of building performance simulations, to quantify the effect of dew, and above-roof air temperature fields, on roof thermal performance. Thus, the importance of these factors in the performance of cool roofs will be identified, and tools will be developed to enable building scientists to easily take them into account in the future.

Introduction

Background

'Cool' roofing materials are engineered to maximise the solar reflectance and thermal emittance of the roof top surface. Cool roofs tend to remain colder than those fabricated from conventional roofing materials, because they reflect a relatively large fraction of incoming short-wave solar radiation, and transmit a relatively large quantity of long-wave radiation to the sky. Such a reduction in surface temperature can reduce the amount of heat transmitted into a building during hot periods, thereby reducing the energy required for space cooling and/or improving the indoor comfort conditions. However, in cold conditions, cool roofs tend to reduce indoor thermal comfort and/or increase the energy required to heat indoor spaces—an effect often referred to as the cool roof 'heating penalty'. Thus, the suitability of cool roof technology depends on the local climate, as well as the building design and usage.

A recently completed research project entitled 'Driving Increased Utilisation of Cool Roofs on Large-Footprint Buildings' (RP1037) investigated previous claims that cool roofs may have additional effects on the performance of buildings with large roof surfaces (e.g. airport terminals and shopping centres) and rooftop heating, ventilation and air-conditioning (HVAC) equipment (Green *et al.*, 2018). In that study, it was confirmed experimentally that, in addition to the effects that cool roofs have on heat transmission through the roof structure, they can also significantly alter the temperature of air surrounding rooftop HVAC equipment. An empirical model was formed that can predict near-roof air temperatures, taking into account the influence of roof surface temperature, and the model was implemented in a set of building performance simulations (BPS). The simulation results indicated that the effect roof surface temperatures have on ventilation air inlet temperatures and rooftop heat exchanger efficiencies can cause changes in annual HVAC electricity and gas consumption of up to 5%. Moreover, in the cases investigated, these above-roof air temperature effects were found to account for approximately half of the benefits and penalties associated with cool roofs. Thus, if the near-roof air temperature field had not been modelled accurately (as is currently the conventional practice in BPS), the cooling savings and heating penalties associated with cool roofs would have been underestimated by approximately 50%.

The findings of RP1037 have provided valuable insight into the magnitude of effect that near-roof air temperatures can have, and the importance of these effects in the performance of cool roofs. The empirical above-roof temperature model has also provided a means for BPS practitioners to take near-roof air temperatures into account. However, the experiments on which the model was based were limited to three buildings and a relatively small set of weather conditions. Therefore, validation of the model with additional experimental data would be highly valuable, and users of the model should have a clear understanding of any limits to the range of conditions which it is valid for. In particular, the validity of the model for use in simulations of cold conditions is of interest, since the experiments were all conducted in warm summer/autumn conditions and the model has a large effect on predicted cool roof heating penalties, which arise in cold conditions. This issue has been investigated in the present work.

The second issue that has been investigated in the research reported here is that of water condensation on roof surfaces, and the effects that this phenomenon can have on the performance of cool roofs relative to roof constructed of more conventional roofing materials. When a roof surface temperature falls below the local dew-point temperature, water will condense on the surface, which could have two potentially significant effects on the thermal performance of roofing materials:

1. The release of latent heat during condensation and absorption of latent heat during evaporation could significantly influence roof surface temperatures.
2. Water droplets or films on the roof surface could significantly alter the roof radiative-optical properties, thereby influencing roof surface temperatures.

Prior to investigation, it was speculated that cool roofs and 'non-cool' roofs could reach very similar temperatures when covered in condensed water, and that this could significantly reduce cool roof heating penalties. In the present study, the authors have quantified the effects of condensation on cool and 'non-cool' roofs, in order to determine whether this could be true.

Aims

The aims of the current project have been outlined below:

1. Quantify the range of weather conditions for which the existing RP1037 above-roof temperature model can be applied, and develop a new model for cold weather conditions if needed.
2. Quantify the effects of condensation on cool roof thermal performance, relative to metal-coated ('non-cool') roofing materials.
3. Revise results from the RP1037 BPS, cost-benefit analysis and greenhouse gas emissions abatement calculations, to take into account any revisions to the above-roof temperature model, and the effects of condensation if they prove to be significant.
4. Ensure utilisation of research outcomes by producing technical design support resources, conducting a series of seminars for key user groups, and disseminating findings in appropriate industry and academic publications.

Method

The project has been divided into four primary activities:

1. Investigate the effects of condensation on cool roof performance, by:

a. reviewing literature related to condensation on roofs and the physical phenomena involved in this process;

b. analysing the existing RP1037 dataset, to determine how often condensation was likely to occur and whether there was a discernible effect on roof surface temperatures at those times;

c. developing a model that can estimate the rate of water condensation and evaporation on a roof surface, as well as the effects of these processes on roof radiative-optical properties and the roof temperature; and

d. conducting dynamic BPS, with and without the condensation model, of buildings with cool and 'non-cool' roofs, to quantify the effect of condensation in several illustrative cases.

2. Address issues related to use of the existing above-roof temperature model in simulations of cold conditions, by:

   a. quantifying the range of weather conditions recorded during the RP1037 experiments and comparing this to the range of conditions predicted throughout a typical year in different Australian climates; and

   b. revising the above-roof temperature model if necessary.

3. Replicate BPS, cost-benefit analysis and greenhouse gas emissions abatement calculations from RP1037, incorporating the condensation model and revised above-roof temperature model, if necessary.

4. Disseminate research findings through publications, seminars, and summary design support resources.

Report outline

This is the first interim report for RP1037u1 'Above-Roof Temperature Impacts on Heating Penalties of Large Cool Roofs in Australian Climates', an extension of the original project, RP1037. Thus, not all of the activities outlined above were complete at the time of writing. In this report, the authors have outlined progress on:

- the literature review;
- analysis of the existing RP1037 dataset to identify the likelihood of roof condensation;
- development of the roof condensation model; and
- analysis of the existing above-roof temperature model.

These three topics constitute the three main sections of the report. A short conclusion has also been included, to summarise the key preliminary findings that have arisen from the research so far.

Literature Review

A review has been presented here, of the potential influences that dew may have on roof thermal performance, and different approaches to quantify these influences. First, previous investigations into water condensation on roofs are discussed, then the two primary mechanisms by which dew can effect roof thermal performance are explored in more detail, namely: i) latent heat release/absorption during the condensation and evaporation processes, and ii) changes in the apparent radiative-optical properties of the roof surface.

Previous work on roof condensation

A number of previous studies have investigated water condensation on roofs. Some of these studies investigated condensation inside the roof cavity, on the internal surface of the roof (Simpson *et al.*, 1992; Essah *et al.*, 2009). Depending on the roof construction and internal conditions, water can condense indoors or between layers of the roof system. Condensation on the roof top/external surface (i.e. dew formation) is influenced only by the outdoor conditions and roof surface temperature. Studies into internal condensation have not been discussed in-detail in this report, and the present study was focused on dew formation on the external roof surface.

A small number of previous studies have investigated water condensation on roof external surfaces (Pieters *et al.*, 1995; Tywoniak, 1999; Richards, 2009; Piscia *et al.*, 2012). Of these studies, it appears that none have taken into account the effect of water droplets and films on roof radiative-optical properties. Furthermore, most of these previous investigations arguably did not adopt the most appropriate convective heat transfer coefficient algorithms for use on roof-like surfaces. Convective heat transfer coefficients are used to calculate mass transfer coefficients, which directly influence calculated condensation and evaporation rates, and thereby, latent heat release/absorption rates. Therefore, the two key effects of dew on roof thermal performance, the heat fluxes caused by the latent heat release and absorption, and changes in radiative-optical properties, may not have been modelled accurately. These previous investigations have been summarised briefly below.

Richards (2009) adapted an existing model, designed to estimate dew accumulation on leaves for the agricultural sector, into an urban dew model for estimation of the quantity of dew that could be harvested from roof surfaces. One of the empirical models from Mcadams (1942) was used to calculate the convective heat transfer coefficient, and thereby predict the latent heat transfer. The emissivity of the roof surface was not modified to account for the effects of dew. Comparison of the model results with experimental data revealed a RMS error of 0.04 mm in terms of the dew thickness accumulated over night, which was significant considering that the mean end-of-night dew thickness was 0.09 mm. One source of error is likely to have been the convective heat transfer model used, which is only applicable for wind speeds lower than 5 m s^{-1}.

Tywoniak (1999) studied water condensation on cold roof surfaces numerically. Dew deposition was allowed on both the internal and external roof surfaces, under the assumption that the sub-roof space was well ventilated (i.e. had equal temperature and humidity as the outdoor space). The release/absorption of latent heat was calculated using a model from Bloudek (1992). However, a convective heat transfer model was adopted that is only applicable to free convection (i.e. conditions with negligible wind). Furthermore, the effects of dew on the apparent emissivity of the roof surfaces were not considered. The model predicted an extremely high total condensation rate..

Piscia *et al.* (2012) carried out a computational fluid dynamics (CFD) simulations, to predict the indoor conditions of a greenhouse, taking into account the effects of condensation on the greenhouse roof. A user-defined function (UDF) was coupled with a commercial CFD package to simulate the film condensation. However, the apparent emissivity of the roof surface was not modified to account for the effects of dew. The results showed that the condensation rate could be represented quite accurately by a logistic function regression, which would vary according to the conditions. However, the CFD results were only validated in terms of the greenhouse indoor conditions, and no evidence was presented that supported the accuracy of simulated dew condensation. Furthermore, the simulation was carried out for a four-span greenhouse roof with a roof pitch of 45º, so the results cannot necessarily be applied directly to large, near-horizontal, opaque roofs.

Pieters *et al.* (1995) modelled the onset of condensation on both the inner and outer surfaces of greenhouse covers. It was found that the use of low emissivity glass can increase the threshold of condensation for both inner and outer surfaces of a greenhouse. However, the modelling was not continued, to investigate the effects of water condensation on the roof thermal performance after condensation had started to form. The convective heat transfer coefficient that was used was not specified.

Latent heat

As water condenses on roof surfaces, it releases latent heat, and as it evaporates, it absorbs the same amount of latent heat. The quantity of latent energy that is released/absorbed per unit mass of water is a well-known quantity referred to the specific heat of vaporisation; it is equal to approximately 2,257 kJ kg^{-1} at atmospheric pressure (Çengel and Boles, 2002). Therefore, if the dew mass transfer rate can be accurately quantified, the significance of latent heat effects on the thermal performance of roofs can be evaluated.

In the BPS software EnergyPlus (EnergyPlus, 2010), an optional setting is available to take into account the latent heat effects of condensation on building external surfaces, without calculating the mass transfer rate. In this approach, an extremely high convective heat transfer coefficient is set for any surface that is below the dew-point temperature, and the outdoor air temperature applied to that surface is artificially set to the dew-point temperature. Thus, external surface temperatures are prevented from falling significantly below the dew-point

temperature. Inherent in this approach are assumptions that: i) the mass transfer rate during condensation is effectively unlimited, so that sufficient latent heat can be released to maintain the surface at the dew-point temperature, and ii) the evaporation process does not have a significant effect surface temperatures. No justification was found in the EnergyPlus documentation for either of these assumptions, and no other evidence was uncovered in this review that appears to justify them.

Some studies have estimated evaporation/condensation rates by performing a statistical regression on experimental data. For instance, a series of regression models were proposed by Maestre-Valero *et al.* (2015) and Beysens *et al.* (2006) to predict dew formation on various surfaces, given different ambient conditions. However, the simplicity of these models was shown to produce considerable errors in predictions of dew accumulation rates (R^2 ranging from 0.27 to 0.57) (Maestre-Valero *et al.*, 2015).

Condensation and evaporation rates can also be deduced theoretically, based on an analogy between convective heat and mass transfer. It has been demonstrated experimentally that these two related processes can be correlated using the Lewis number (Bergman *et al.*, 2011). Thus, if the convective heat transfer coefficient can be estimated accurately, it can be used to calculate the convective mass transfer coefficient (Tiwari *et al.*, 1982; Keller, 1985; Beysens *et al.*, 2005; Richards, 2009; Monteith and Unsworth, 2013). Therefore, it is important that a convective heat transfer coefficient correlation that is accurate for roofs is used, if accurate condensation/evaporation estimates are to be attained via this method.

Many correlations have been recommended for the estimation of convective heat transfer at the external surfaces of buildings, and several researchers have compared them (Mirsadeghi *et al.*, 2013; Costanzo *et al.*, 2014). Many of the correlations were based on laboratory-scale experiments and have not been validated for building-scale surfaces, so it is unclear whether they are valid for such large length scales. Furthermore, the 'completeness' of the different correlations, in terms of the set of relevant physical factors that they take into account (e.g. surface orientation, surface size, surface roughness, air flow turbulence characteristics, roof/air temperature difference, etc.), varies widely. A selection of the most relevant correlations have been described below.

Duffie and Beckman (2013) presented a range of convective heat transfer correlations, but recommended one model, based on work by Mitchell (1976), for use on large building-scale surfaces in outdoor conditions. This model combines an empirical correlation for forced convection conditions with a minimal value of 5 W m^{-2} K^{-1} which applies to natural convection as long as the wind speed is lower than 5 m s^{-1}.

Mirsadeghi *et al.* (2013) summarised and compared a number of external convective heat transfer coefficient models that were in common use in BPS programs. The most 'complete' models were the 'BLAST'-related models (including the 'TARP' model), the 'MoWitt' model and the 'DOE-2' model. However, the BLAST-related models do not appear to have been thoroughly validated for building-scale surfaces, and the MoWitt model was developed based on vertical building surfaces, so may not be valid for roofs.

A convective heat transfer model developed by Krisher and Kast (which was used by Holck and Svendsen (2004) for latent heat flux calculation) takes the difference between laminar and turbulent flow into account. The 'completeness' of this model was high; however, the range of applicability of this model was not clearly stated.

Costanzo *et al.* (2014) compared a number of commonly used convective heat transfer coefficient models to field measurements from a flat roof in Italy. Results obtained using the different models deviated from each other considerably. The 'ClearRoof' model, proposed by Clear *et al.* (2003), reproduced the experimental data most accurately, followed by the TARP model.

Of the models reviewed here, the ClearRoof model is one of the most 'complete'. Furthermore, it was developed for use in relation to the horizontal roofs of commercial buildings, and further validated for such surfaces by Costanzo *et al.* (2014). It is not clear to the present authors whether the treatment, within the ClearRoof model, of above-roof air flow as laminar when the reference wind speed is below a certain threshold is valid, since the sharp leading edge of the roof surface is likely to 'trip' flow into a turbulent state. This has been documented in many studies of air flow around buildings (Castro and Robins, 1977; Richards *et al.*, 2007; Blocken *et al.*, 2013). Nevertheless, the ClearRoof model has accurately reproduced two sets of experimental results from full-scale flat-roofed buildings in real wind, so it appears to be one of the most suitable models available for such cases.

Influence on radiative-optical properties

Thermal emittance

It has been reported in a number of studies that the presence of water droplets or films on a surface can influence the long-wave radiant heat transfer to/from the surface significantly (Lee *et al.*, 2016). Robinson *et al.* (1957) used a guarded hot box to measure changes in the thermal resistance of a reflective foil surface as water condensed on the surface. When condensed water was observed to cover approximately 10% of the foil area, the foil thermal resistance was reduced by 10-30%. They attributed the phenomenon to the high emittance of water film, even when it was only a few thousandths of an inch thick.

Bassett and Trethowen (1984) also investigated the effect of condensed water on the emittance of reflective insulation surfaces. They found that condensate loadings of 1 g m^{-2} (1 μm mean thickness) increased the apparent emittance of aluminium foil from 0.06 to 0.25. It was noted that the apparent emittance did not immediately rise to that of a bulk water when water was present, but increased gradually with increasing condensate thickness. This could be explained by the infrared transmittance of a water film being non-zero (i.e. while water is a strong absorber in the infrared, it is not entirely

opaque). It was also observed that, when the condensate mass loading was maintained at 0.92 and 0.55 g m^{-2} over a period of more than 5 days, the apparent emissivity decreased slightly within the first 24 h (by 0.03 and 0.15, respectively), but afterwards little change was observed. It was suggested that this change could have been caused by droplet coalescence, which would alter the fraction of the surface that is covered by water and the depth of the water layer.

Mao and Kurata (1998) conducted experiments into the influence of condensation on the thermal performance of porous sheets used to cover agricultural crops. The results revealed that the apparent emissivity of the row cover materials increased from 0.26 to approximately 0.45, given dew deposition of 0-40 g m^{-2}.

Ambrose and Karagiozis (2007) numerically evaluated the thermal benefits of using a pressure-equalized insulated glass unit (IGU) in building envelopes. In the simulations, the effect of condensed water on the apparent emissivity of glass panes with low-emission coatings was modelled using outcomes from the experiments carried out by Bassett and Trethowen (1984). It is possible that a similar approach can be taken in the investigation of roof surfaces.

Solar reflectance

It has been reported that the solar (i.e. short-wave) reflectance of glazed photovoltaic panels at a perpendicular incidence angle can be about 4-5%, due to the high refractive index of the glass layers (Krauter, 2004). Similarly, when dew exists on a roof surface, it acts as a reflective layer. However, since water has a lower refractive index than glass, 1.33 vs. ~1.5 (Hosseini *et al.*, 2019), the reflection loss is smaller. According to the Fresnel equation, the solar reflectance of a water film at a perpendicular incidence angle is around 2–3%.

Surface soiling

It has been suggested that dew can cause dust to accumulate on roof surfaces, thereby gradually changing the roof surface radiative-optical properties over time (Ilse *et al.*, 2019). As was identified in RP1037, the soiling of roof surfaces can affect their thermal performance significantly. However, it is likely that any contribution dew has in the ageing/fouling of roofing materials is already accounted for in the empirical models used to predict these effects (Sleiman *et al.*, 2011, 2014; Paolini *et al.*, 2014).

Condensation likelihood in the RP1037 dataset

Experimental data collected in RP1037 includes over 18 weeks of roof surface temperature and local dew-point temperature measurements. Three case study shopping centres were studied; roof surface temperatures were measured at 15 locations on each roof and the dew-point temperature was measured at the top of an 8m-tall mast, near the centre of each roof. While condensation was not measured directly, any measured roof surface temperature equal to, or lower than, the corresponding dew-point temperature indicates that roof condensation was likely at that time.

The spatially averaged roof surface temperature, T_s, dropped below the dew-point temperature, T_{dp}, on approximately 80% of nights, at each of the three buildings studied (see an example of a typical 24 h period in Figure 1 and a summary of all measurements in Figure 2). When this occurred, T_s often reached temperatures several degrees below T_{dp}, for several hours. Two conclusions can be drawn from these observations: i) water is likely to have condensed on the roof surfaces on most nights during the monitoring periods, and ii) the latent heat released during the condensation process was insufficient to keep the roof surface temperatures at or above the dew-point temperature. Whether or not the condensed water had a significant effect on roof surface temperatures cannot be determined from the RP1037 dataset alone, so a new condensation model has been developed and applied in the subsequent sections of this report, to quantify such effects.

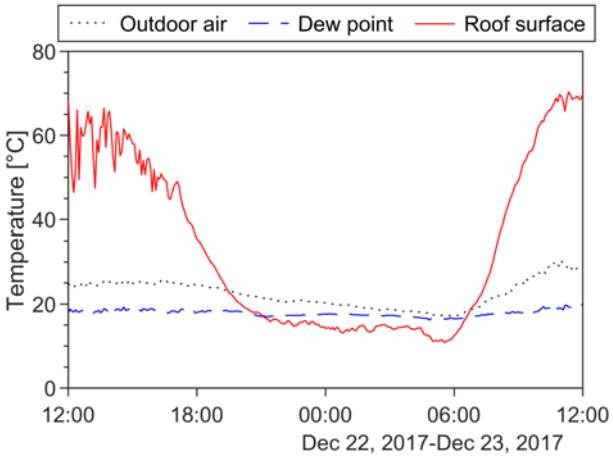

Figure 1: Comparison of outdoor air, dew point and spatially averaged roof surface temperatures, measured through a typical 24h period during the experiments.

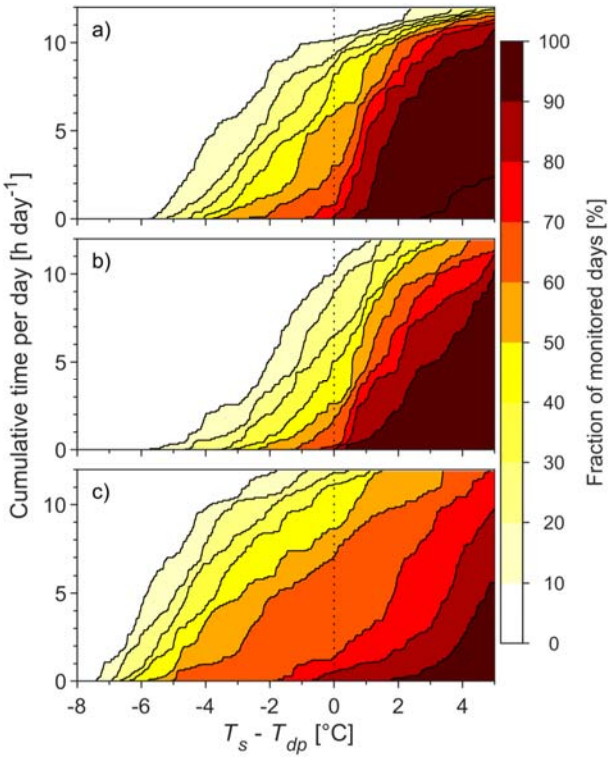

Figure 2: Time in which the mean roof surface temperature, T_s, was below the local dew point temperature, T_{dp}, during experiments at a) Nowra, b) Shellharbour, and c) Wetherill Park.

Roof condensation model

This section of the report describes the development and verification of a model that can simulate the water condensation/evaporation process on a roof surface. Several numerical case studies have also been presented, to demonstrate the influence of key variables under quasi-steady conditions.

Model development

Energy balance

The energy balance of a flat roof sheet is illustrated in Figure 3. Accordingly, the governing equation for the energy balance of a roof can be expressed using Equation 1, given the assumptions listed below:

- Heat transfer to/from the roof sheet lower surface is via conduction only (e.g. through a layer of insulation);
- The heat capacitance of dew formed on the roof surface is negligible;
- The roof sheet and any accumulated dew are isothermal; and
- The roof surface radiative transmittance is zero (i.e. it is opaque).

$$c_{p,s} m_s \frac{dT_s}{dt} = \alpha_s G_t - q''_{conv} - q''_{lat} - q''_{rad} - q''_{cond} \quad (1)$$

Here, $c_{p,s}$ is the specific heat capacity of the roof material, m_s is the roof sheet mass per unit area, T_s is the roof surface temperature, t is time, α_s is the roof surface solar absorbtance, G_t is the solar heat flux incident on the roof surface, and q'' is a heat flux from the roof sheet; subscripts 'conv', 'lat', 'rad' and 'cond' signify convective, latent, radiative and conductive heat transfers, respectively. Equation 1 can be discretised, which allows the roof surface temperature to be calculated through a series of discrete time steps.

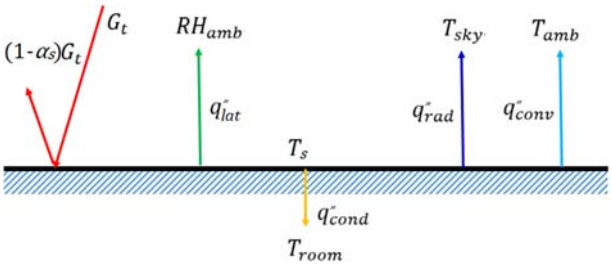

Figure 3: Energy balance of a flat roof.

External convective heat transfer

The convective heat flux from the external surface of the roof can be calculated using the expression:

$$q''_{conv} = \bar{h}_{conv}(T_s - T_{amb}) \quad (2)$$

where the $\bar{h}_{conv}$ is the spatially averaged convective heat transfer coefficient. Five of the most suitable models for $\bar{h}_{conv}$ have been compared in Figure 4, including the: i) ClearRoof model (Clear *et al.*, 2003), ii) model developed by Krisher and Kust (Holck and Svendsen, 2004), iii) TARP model (Walton, 1981), iv) DOE-2 model (LBL, 1994), and v) model developed by Mitchell (1976). Detailed descriptions of these models can be found in the corresponding references, so they have not been included here. The parameters used in the model comparison are summarised in Table 1; they represent two large (70,000m^2) roofs, with different length-to-width aspect ratios. The ASHRAE roughness factor and terrain roughness category were required by some of the models; values representing a relatively smooth roof surface within an urban terrain have been adopted here. For more details regarding these parameters, the interested reader is directed to ASHRAE (2009) and (Walton, 1981).

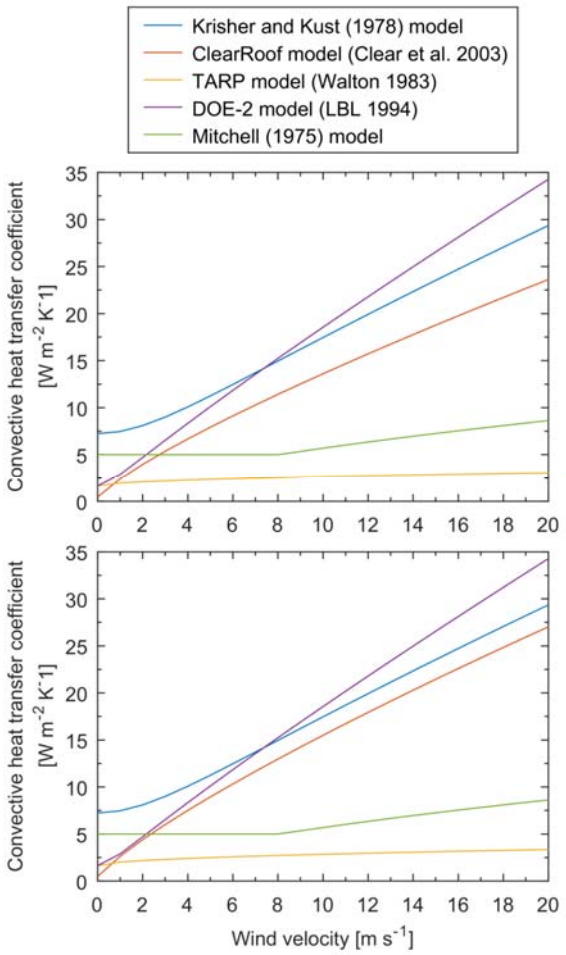

Figure 4: Comparison of external convective heat transfer coefficients calculated using different models, for a) Roof A, and b) Roof B.

Table 1: Summary of parameters used for the comparison of the external heat transfer coefficients calculated using different models.

Parameter	Roof A	Roof B
Roof surface temperature (T_s) [°C]	10	10
Ambient air temperature (T_{amb}) [°C]	20	20
Roof length (L) [m]	350	700
Roof width (W) [m]	200	100
Height above ground (H) [m]	10	10
Reference wind speed (u_{ref}) [m s^{-1}]	0–20	0–20
Wind direction relative to the normal of the roof length (θ) [°]	0	0
ASHRAE roughness factor (R_f)	1	1

The ClearRoof model, Krisher and Kust model, and DOE-2 model produced results that were fairly similar in the cases investigated; the TARP model and Mitchell model gave much lower $\bar{h}_{conv}$ values for wind speeds greater than 5 m s^{-1}. The obvious deviations indicated the importance to select an appropriate model to calculate the convective heat transfer coefficient. Previous studies have validated the ClearRoof model (Costanzo et al. 2014) and concluded that it was relatively accurate for near-horizontal roofs. The ClearRoof model is also takes into account many of the physical parameters that are important in the convective heat transfer process, e.g. roof surface roughness, roof size and wind direction. For these reasons, the ClearRoof model was adopted to determine $\bar{h}_{conv}$ in the roof condensation model developed here.

Latent heat transfer

The rate of latent heat released during condensation, and absorbed during evaporation, can be calculated as follows (Holck and Svendsen, 2004):

$$q''_{lat} = \dot{m}_{evap}\gamma = h_m \rho_{air} \frac{M_{water}\gamma}{M_{air}P_0}\left(P_{ws}|_{T_s} - P_{ws}|_{T_{dp}}\right) \quad (3)$$

where $\dot{m}_{evap}$ is the mass transfer rate per unit area, γ is the latent heat of vaporisation of water, h_m is the convective mass transfer coefficient, ρ_{air} is the density of air, M_{water} and M_{air} are the molecular weights of water and air, respectively, P_0 is the total barometric pressure, P_{ws} is the water vapour saturation pressure, and T_{dp} is the dew-point temperature. In the present work, $\dot{m}_{evap}$ is defined as positive for evaporation and negative for condensation.

Mass transfer of water to/from a surface via condensation/evaporation is similar to convective heat transfer, in terms of the limiting convection and diffusion processes that are involved. It has been shown that h_m is approximately proportional to $\bar{h}_{conv}$ and that one coefficient can be calculated from the other using the Lewis number, Le (Bergman *et al.*, 2011):

$$h_m = \frac{\bar{h}_{conv}}{\rho_{air} c_{p,air} Le^{1-n}} \quad (4)$$

Here, $c_{p,air}$ is the specific heat capacity of air. Bergman *et al.* (2011) demonstrated that it is assumed to a value n = 1/3 for the mast of the applications, and a value of Le = 0.9 was used for water condensing from air (Holck and Svendsen, 2004).

If it is assumed that the physical properties of air and water are approximately constant in the range of temperatures that are of interest, substitution of appropriate values for γ, M_{water}, M_{air}, $c_{p,air}$, P_0 and Le into Equations 3, and combination with Equation 4, yields (Holck and Svendsen, 2004):

$$q''_{lat} \approx \begin{cases} 0.017\bar{h}_{conv}\left(P_{ws}|_{T_s} - P_{ws}|_{T_{dp}}\right) & T_s \geq 0 \\ 0.019\bar{h}_{conv}\left(P_{ws}|_{T_s} - P_{ws}|_{T_{dp}}\right) & T_s < 0 \end{cases} \quad (5)$$

External long-wave radiative heat transfer

The long-wave radiative heat transfer between the roof and the sky can be calculated using the expression:

$$q''_{rad} = \varepsilon_{eq}\sigma\left(T_s^4 - T_{sky}^4\right) \quad (6)$$

where T_{sky} is the sky radiative temperature, σ is the Steffan Boltzmann constant, and ε_{eq} is the apparent roof surface emissivity. T_{sky} can be estimated for clear (i.e. non-cloudy) conditions, at altitudes close to sea-level, as (Martin and Berdahl, 1984):

$$T_{sky} \approx T_{amb}\left(0.771 + 0.0056T_{dp} + 0.000073T_{dp}^2 + 0.013\cos\left(\frac{2\pi}{24}t_h\right)\right)^{0.25} \quad (7)$$

where t_h is the hour of day (starting at 0, at midnight). T_s, T_{sky} and T_{amb} must be expressed in Kelvin in Equations 6–7, and T_{dp} must be expressed in degrees Celsius.

If it is assumed that condensed water on the roof surface forms a film of uniform thickness, the apparent roof surface emissivity, ε_{eq}, depends on the dry roof emittance, ε_s, and the water film thickness, δ. In the roof condensation model developed here, ε_{eq} is estimated using the following expression (Xu and Shen, 1992):

$$\varepsilon_{eq} = \begin{cases} \varepsilon_s, & \text{for dry roof} \\ \frac{(1-\rho_{water})[1-\rho_s exp(-2\alpha_A\delta)]}{1-\rho_s\rho_{water}exp(-2\alpha_A\delta)}, & \text{for wet roof} \end{cases} \quad (8)$$

Here, α_A is twice the Lambert absorption coefficient, ρ_{water} is the reflectance for long-wave radiation arriving from the water side, and ρ_s is the reflectance of the roof-water interface, which is equal to $(1 - \varepsilon_s)$. The value used for α_A in the present study was 0.1184, which represents the mean value averaged over an infrared range from 8×10^2 nm to 3×10^5 nm (ZOLOTAREV and VM, 1969; Hale and Querry, 1973; Downing and Williams, 1975). The value of ρ_{water} was set as 0.04, which is the hemispherical average infrared value integrated from data reported by Sidran (1981).

In order to assess the validity of the apparent emissivity model in Equation 8, experimental data from Bassett and Trethowen (1984) was compared to the model (see Figure 5). The modelled and measured values agreed very well in this case, involving a low-emissivity foil surface, with a root mean square error (RMSE) of 0.0354.

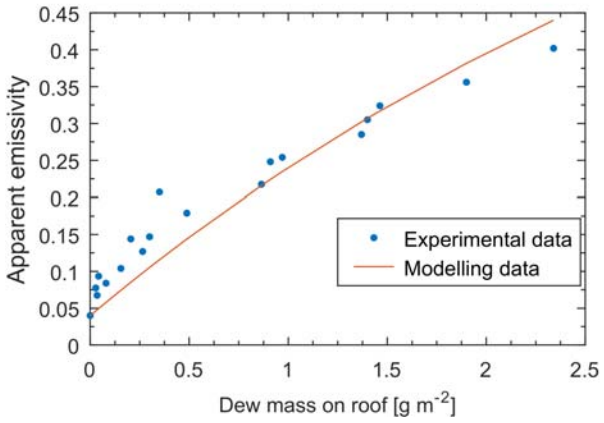

Figure 5: Comparison of the apparent emissivity model with experimental data.

The effect of a water film on the effective thermal emittance of three typical roofing materials is illustrated in Figure 6. It can be seen that a dramatic change can occur with small changes in the dew condensation, when it is lower than 10 g m^{-2} (i.e. when dew water film thickness $\delta \lesssim 10$ μm). For thicker water films, the effective surface emittance approaches the emissivity of a limit for bulk water, which appears to have been effectively reached for dew mass loadings above 20 g m^{-2} (i.e. dew water film thickness $\delta \gtrsim 20$ μm).

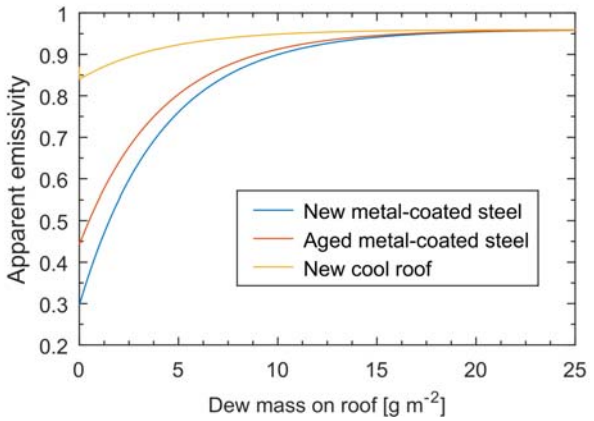

Figure 6: Effect of a water film on the apparent thermal emittance of roof surfaces.

External short-wave radiative heat transfer

Short-wave (i.e. solar) radiative heat transfer has not been included in the roof condensation model for two reasons: i) roof condensation predominantly occurs at night, when there is no significant short-wave radiative transfer, and ii) water films have been shown to have a relatively small effect (~2-3% for solar radiation from normal direction) on the effective short-wave absorbtance of surfaces.

Conductive heat transfer below roof

Heat transfer from the roof sheet to the indoor environment can be approximated as:

$$q''_{cond} = U(T_s - T_i) \quad (9)$$

where T_i is the indoor air temperature, and U is the overall thermal conductance between the roof sheet and the indoor environment. U can be calculated from the internal convective heat transfer coefficient, h_i, and the thermal resistance of the roof structure below the roof sheet, R_s:

$$U = 1/(R_s + 1/h_i) \quad (10)$$

In this simplified approach, radiative heat transfer within the building is neglected. This simplification should not have a large effect on results for well-insulated roofs, and when the model is implemented in BPS, the simulation software will account for radiation within the building.

Model integration

By combining Equations 1, 2, 5, 6, 7, 8, 9 and 10 with the ClearRoof model, and establishing a set of boundary conditions (including T_{amb}, RH_{amb}, T_i, G_t, α_s, ε_s, m_s, $c_{p,s}$, t_h, the roof dimensions, roof surface roughness, reference wind speed (u_{ref}) and wind direction(θ)), changes in the water condensation rate and the roof surface temperature over time can be estimated. In the present work, the Euler method was used to solve the discretised differential equations.

Quasi-steady case studies

To investigate fundamental aspects of the condensation/evaporation process of dew on a roof, several quasi-steady cases were simulated using the roof condensation model. Three simulations were run with the steady boundary conditions summarised in Table 2. In one the effects of dew on the roof energy balance were not included at all, in the second only the effects of dew on apparent emissivity were included, and in the third both emissivity and latent heat effects were included. Simulations were then run with a range of ambient air temperatures and humidities (ranging from 12°C to 22°C and 70% to 90%, respectively), to investigate the effect of these parameters on dew condensation process.

Table 2: Steady boundary conditions used in the modelling.

Parameter	Value
Initial roof surface temperature ($T_{s,initial}$) [°C]	10
Ambient air temperature (T_{amb}) [°C]	20
Ambient relative humidity (RH_{amb}) [%]	80
Indoor air temperature (T_i) [°C]	20
Roof length (L) [m]	350
Roof width (W) [m]	200
Height above ground (H) [m]	10
Reference wind speed (u_{ref}) [m s^{-1}]	10
Wind direction relative to normal of the roof length (θ) [°]	0
ASHRAE roughness factor (R_f)	1
Terrain roughness category	4
Dry-roof emissivity (ε_s)	0.85
Overall thermal conductance between the roof sheet and the indoor environment (U) [W m^{-2} K^{-1}]	0.5
Roof mass per unit area (m_s) [kg m^{-2}]	3.959
Specific heat capacity of the roof ($c_{p,s}$) [kJ kg^{-1} K^{-1}]	0.5
Barometric pressure (P_0) [kPa]	101.325
Time of day (t_h) [h]	0
Latent heat of vaporisation (γ) [kJ kg^{-1}]	2500

Effects of condensation

Figure 7 presents results from the thermal balance process. It can be seen from Figure 7a that the roof temperature increased rapidly in this case, before decreasing gradually towards a limit, where thermal equilibrium was reached. The dew condensation rate also approached a limit; however, the limit was greater than zero, so the water film thickness was steadily increasing with time.

The two primary mechanisms by which roof condensation can effect roof temperatures are explored in Figure 7b. The overall effect of roof condensation on the quasi-steady roof temperature was only 0.03°C. However, rapid condensation in the early phase of the simulation did produce a temporary difference in roof temperature of up to 0.49°C, as compared to the case in which condensation effects were not included. When only the effect of condensed water on the apparent roof emissivity was included (i.e. when the release and absorption of latent heat were ignored), a quasi-steady roof temperature was reached that was 0.3°C lower than that reached without any condensation effects. Under the steady boundary conditions investigated in this case, it seemed that the effects of the roof condensation on the apparent roof emissivity and the release/absorption of latent heat cancelled each other out to some extent; however, both effects seemed to be significant. Given other steady boundary conditions or dynamic boundary conditions, the two effects could combine to affect roof temperatures significantly.

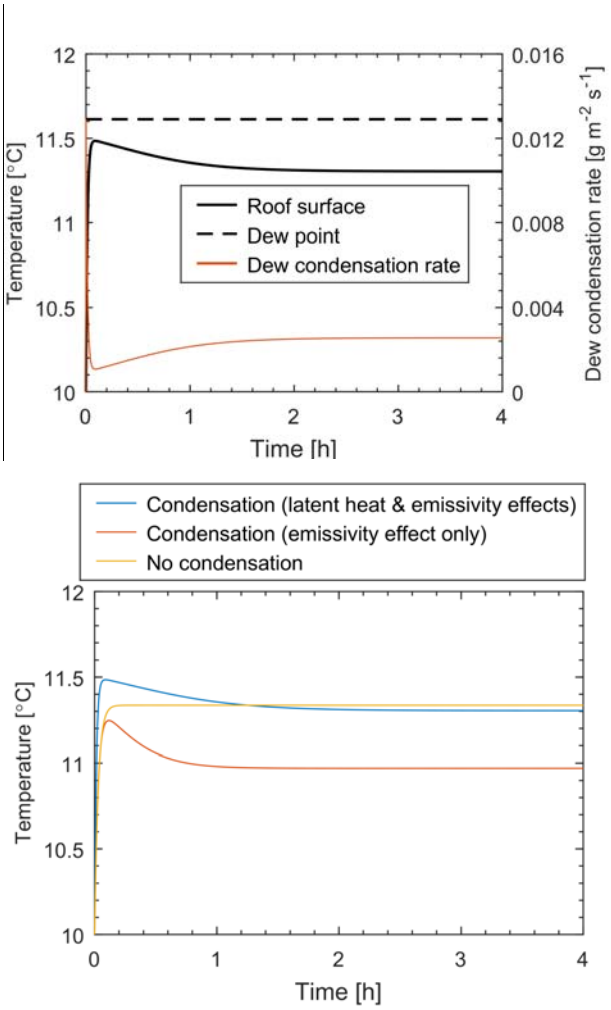

Figure 7: Modelling results for Baseline case: a) for roof surface temperature, and b) for comparison of the roof surface temperatures considering different effects.

Influence of ambient humidity

Figure 8 presents the quasi-steady roof temperature reached after 4 simulated hours, given various levels of ambient humidity. It can be seen from Figure 8a that higher roof temperatures tended to be reached when the ambient humidity was increased. In cases where a roof surface temperature less than the dew-point temperature was reached, condensation continued to occur in the quasi-steady state, which influenced the trend between roof temperature and ambient humidity.

Figure 8b compares the quasi-steady roof temperatures from Figure 8a with those obtained without any roof condensation effects, and with the condensation effects on roof emissivity only (i.e. neglecting the release and absorption of latent heat). It is evident that it is the latent heat release during condensation that has effected the slope of the roof temperature plot in Figure 8a. The effect of a water film on the roof thermal emittance also had a significant effect on quasi-steady roof surface temperatures, but it seemed that the magnitude of that effect did not depend on the ambient humidity. It is also

evident in Figure 8 that water condensation can have a significant effect on roof temperatures in some conditions (around 0.83°C in the cases studied here).

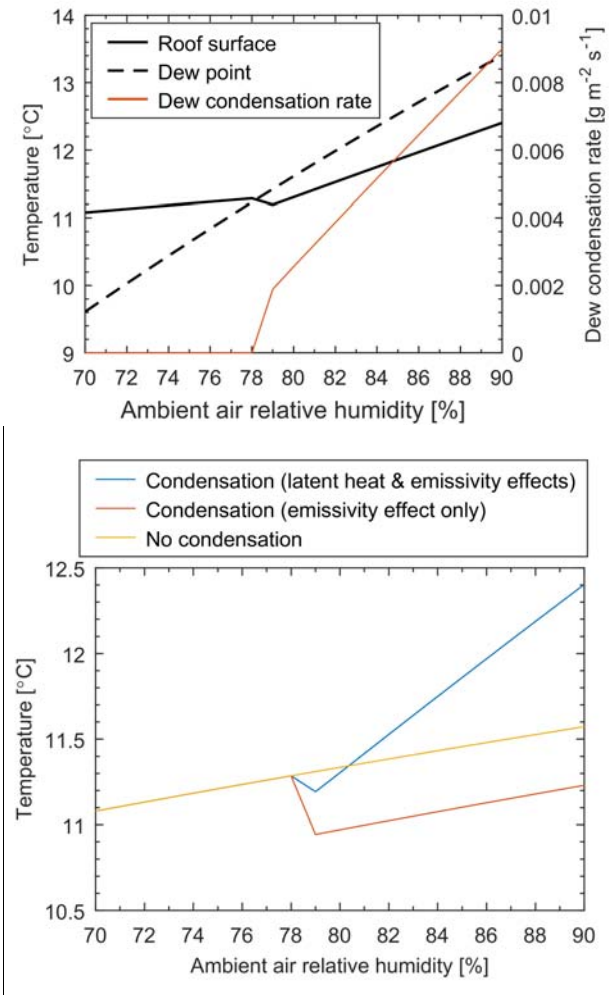

Figure 8: Effect of ambient humidity on the quasi-steady conditions reached after 4 simulated hours: a) temperatures and the condensation rate, and b) temperatures, given different condensation effects.

Influence of ambient air temperature

Figure 9 presents the effect of the ambient air temperature on the quasi-steady roof temperature and condensation rate (see Figure 9a) and heat fluxes (see Figure 9b) that were reached after 4 simulated hours. The magnitude of the condensation rate was driven by the difference between the roof surface temperature and dew-point temperature; for ambient air temperatures above 20°C, the roof surface temperature rose above dew-point, so the condensation rate went to zero. Latent heat fluxes were significantly smaller than convective and radiative heat fluxes in the cases investigated. If the dry-roof emittance had been significantly lower than the bulk-water emittance (e.g. if it had been a metal-coated steel roof), it could be expected that the effects of condensation on the radiative heat flux would be much larger than the latent heat effects in these cases.

Extension of this work to transient boundary conditions, and a variety of roof types, will reveal such details more clearly.

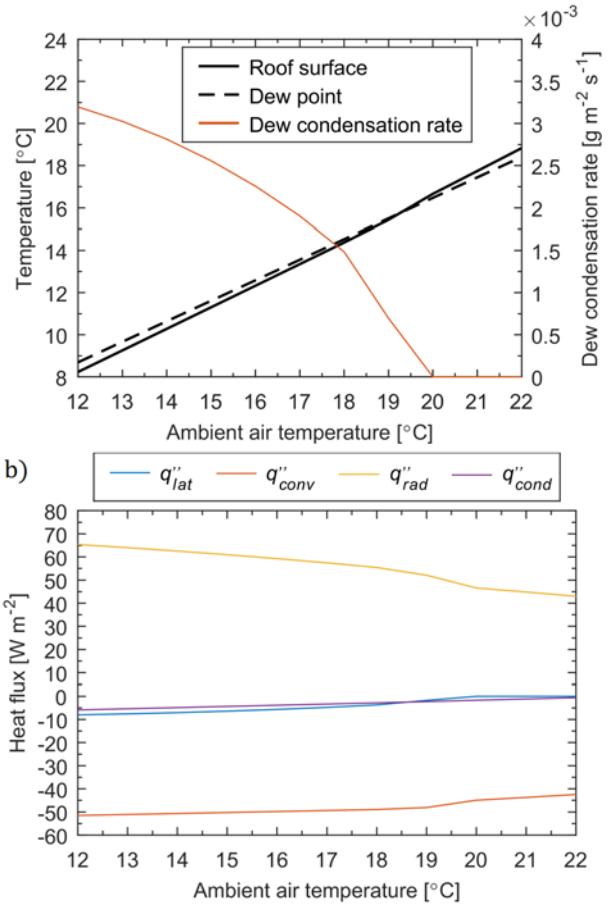

Figure 9: Effect of ambient air temperature on the quasi-steady conditions reached after 4 simulated hours: a) temperatures and the condensation rate, and b) heat fluxes.

Above-roof temperature model

The air temperature field above a roof surface is the product of surrounding air temperatures, the roof surface temperature, and air flow, which can be driven by inertial (i.e. wind) and buoyant (i.e. thermal) forces. Heat will diffuse between the roof surface and air in contact with that surface. The vertical transport of heat, via diffusion and convection, will then produce a distribution of air temperatures between the surface and a 'reference height', where the effect of the roof surface temperature is small enough for the local air temperature to be considered equal to the reference 'ambient' air temperature. It is desirable to be able to predict such vertical temperature profiles, so that realistic inlet air temperatures can be assigned to rooftop HVAC equipment in BPS.

The empirical above-roof temperature model developed in RP1037 predicts air temperatures near a roof surface, given four input variables: i) a reference wind speed, u_{ref}, ii) the mean roof surface temperature, T_s, iii) the 'ambient' air temperature, T_{amb}, and iv) a roof length scale, L (Green *et al.*, 2018). It is based on the premise that the vertical temperature profile above a roof surface will be approximately logarithmic, varying from the roof surface temperature at the roof surface to the 'ambient' air temperature at a reference height.

To the best of the authors' knowledge, the experimental dataset on which the model was based (and which was developed in RP1037) is much more comprehensive than those produced in previous investigations of above-roof air temperature fields (e.g. Leonard and Leonard (2006); Wray and Akbari (2008); Carter (2011); Pisello *et al.* (2013); Carter and Kosasih (2015)), in terms of the number of measurements that were taken, the set of meteorological parameters that were measured locally, and the number of experimental sites that were studied. However, the RP1037 experiments did include only three shopping centre buildings, and the relatively warm weather conditions that occurred near Sydney, Australia, during the period December 2017–May 2018. It is important that any limitations in the validity of the model, which may arise from the limited scope of this dataset, be well understood.

Applicability of the model to cold weather

Since the above-roof temperature model predicts the response of an air temperature field to a hot or cold roof surface, and wind, the parameters that define the range of weather conditions on which it has been based are: i) the difference between roof surface temperature and 'ambient' air temperature, $T_s - T_{\mathrm{amb}}$, and ii) the reference wind speed, u_{ref}. While many other parameters do affect near-roof air temperatures (e.g. the solar heat flux, roof insulation or degree of cloud cover), they do so indirectly, via the effect that they have on u_{ref} or $T_s - T_{\mathrm{amb}}$.

Figure 10 compares the range of $T_s - T_{\mathrm{amb}}$ and u_{ref} covered by the RP1037 experimental dataset with those simulated in the RP1037 BPS. The simulated T_{amb} and u_{ref} values came from reference meteorological year weather files for seven Australian cities, representing seven of the eight primary Australian climate zones defined in the Australian National Construction Code (Australian Building Codes Board, 2016), and the simulated T_s values were calculated during simulations of the shopping centre building model, developed in RP1037, in those climate zones (Green *et al.*, 2018). The parameter bounds presented for each climate zone in Figure 10 include the combined set of T_s values from simulations of the shopping centre with a new cool roof, a new metal-coated roof and an aged metal-coated roof, throughout the entire simulated year.

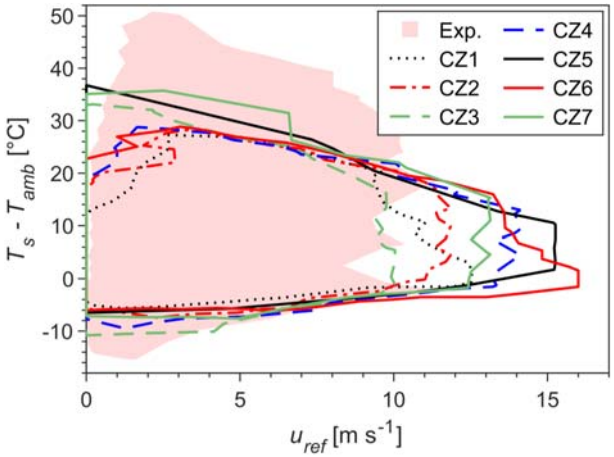

Figure 10: Comparison of the range of conditions that occurred during the experiments in RP1037 (labelled 'Exp.'), with those from year-long building performance simulations of a shopping centre in seven Australian climate zones (labelled 'CZ1'–'CZ7').

Even though the RP1037 experiments were undertaken in relatively warm conditions (near Sydney, in summer and autumn), the wide range of weather conditions included in the year-long simulations of seven climate zones (including many examples of cold winter weather) did not give rise to combinations of $T_s - T_{\mathrm{amb}}$ and u_{ref} that were far from those that occurred during the experiments, except for high wind speeds of $u_{ref} \gtrsim 10$ m s^{-1}. This result supports the validity of the above-roof temperature model in such simulations. The lack of high wind speeds in the experimental dataset indicates that the model can currently only provide near-roof air temperature predictions for such conditions with a relatively large degree of uncertainty. Further validation of the model in these (and indeed, all) conditions would be valuable. However, the effect of any model inaccuracy at high wind speeds on simulated annual HVAC energy consumption would be relatively small in the cases investigated here and in RP1037, since: i) wind speeds over 10 m s^{-1} were very uncommon in the simulations (see Figure 11); and ii) near-roof air temperatures tend to deviate less from the 'ambient' air temperature in strong winds, as the roof surface is brought closer to the 'ambient' temperature by enhanced convective heat transfer, so the model has a relatively small effect on HVAC performance in these conditions anyway.

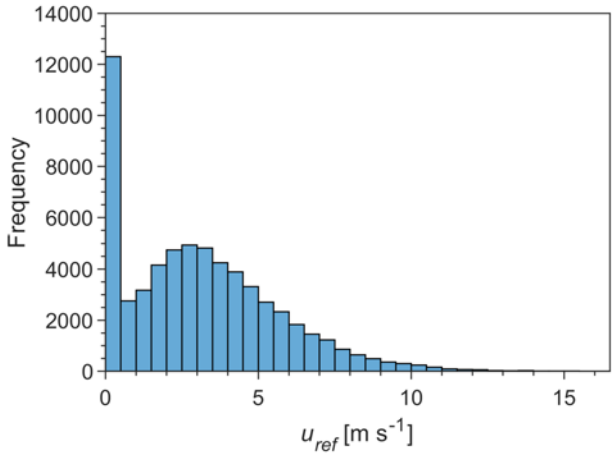

Figure 11: Histogram showing the occurrence of different wind speeds in reference meteorological year weather files for cities in climate zones 1–7.

Applicability of the model to other buildings

The RP1037 experimental dataset was collected from three case-study shopping centre buildings, so care should be taken when applying the above-roof temperature model to buildings or settings much different than those case-studies. Parameters that are likely to have a significant effect on air temperature fields above roofs include:

- Roof size;
- Roof aspect ratio;
- Roof slope;
- Building height; and
- Topography surrounding the building.

The three case-study buildings had roof areas in the range 15,000–77,000 m^2, with aspect ratios less than 3. Although the above-roof temperature model does account for roof size to some degree, it is currently not possible to determine whether it produces accurate results for buildings with roof areas far outside this range, or high aspect ratios. All three buildings had low-angle (<5° from horizontal) roofs, so the model may not accurately predict temperature profiles above roofs with a significantly higher slope. The case-study buildings were approximately 5–20 m tall and were not in close proximity to any taller buildings that could significantly alter incoming wind flow. Therefore, the above-roof temperature model may not be appropriate for use in simulations of tall buildings, or buildings located near large obstructions to air flow.

Experimental measurements of air temperatures above the roofs of more buildings, and the local meteorological conditions, would be highly valuable since they would allow these unknown aspects of the above-roof temperature model to be better understood. Until this has occurred, care should be taken in applying the empirical model to buildings much different from those described above.

Revision of the above-roof temperature model

While conducting the analysis of the RP1037 data described above, it was recognised that a superior fit to experimental data could be achieved by altering the mathematical form of the above-roof temperature model slightly. Thus, an improved above-roof temperature model has been developed and presented here.

The primary change that has been made is in the equation for the shape parameter, α, in unstable conditions (i.e. when $T_s > T_{amb}$). In the old model, α was a function of the Richardson number, Ri (see Equation 11), only, whereas in this new version of the model, α is allowed to vary with $T_s - T_{\mathrm{amb}}$ and u_{ref} independently. A planar surface was fitted to the unstable data, using a least-squares technique. This change reduced the RMS deviation between modelled and measured air temperatures in unstable conditions from 0.83°C to 0.56°C. The new model is described by Equations 11–14, and Figure 12 presents the fit of the new model to the RP1037 experimental data.

$$Ri = \frac{g\beta(T_s - T_{amb})L}{u_{ref}^2} \tag{11}$$

$$\alpha = \begin{cases} -8.983 + 0.03607u_{ref} - 0.2205(T_s - T_{amb}) & Ri \geq 0 \\ -13.08 & -10^{-0.51} \leq Ri < 0 \\ -9.025 + 4.055\sin\left(\frac{\pi}{2}(\log_{10}(-Ri) - 0.64)\right) & -10^{1.79} \leq Ri < -10^{-0.51} \\ -4.97 & Ri < -10^{1.79} \end{cases} \tag{12}$$

$$T_{HVAC} = \frac{1}{z_2 - z_1}\int_{z_1}^{z_2}\left(T_s - (T_s - T_{amb})\frac{\ln\left(\frac{z+10^{\alpha}}{10^{\alpha}}\right)}{\ln\left(\frac{8+10^{\alpha}}{10^{\alpha}}\right)}\right)dz \tag{13}$$

$$T_{HVAC} = T_s - \frac{(T_s - T_{amb})}{(z_2 - z_1)\ln\left(\frac{8+10^{\alpha}}{10^{\alpha}}\right)}\left[(z_2 + 10^{\alpha})\ln\left(\frac{z_2+10^{\alpha}}{10^{\alpha}}\right) - z_2 + z_1 - (z_1 + 10^{\alpha})\ln\left(\frac{z_1+10^{\alpha}}{10^{\alpha}}\right)\right] \tag{14}$$

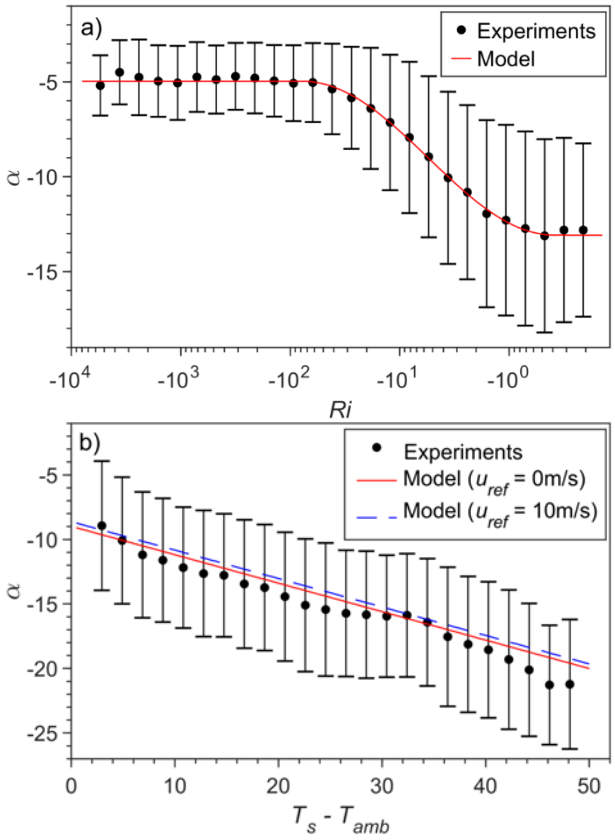

Figure 12: Comparison of the thermal boundary layer shape parameter, α, obtained from experimental data with those predicted by the above-roof temperature model, in a) stable and b) unstable conditions. Experimental data has been represented by the mean (dot) and standard deviation (whiskers) of α within discrete bins.

Conclusion

Two thermodynamic processes that could significantly affect the performance of cool roofs have been investigated: i) the effect of water condensation and evaporation on the roof temperature, and ii) the effect of the roof temperature on above-roof air temperatures, and thereby, on rooftop HVAC equipment. Neither of these processes were taken into account by conventional BPS practices at the time of writing.

A review of literature related to roof condensation, and the relevant physical processes, revealed that the heat fluxes caused by the latent heat release and absorption and the changes in the radiative-optimal properties are the two key effects of dew condensation on the thermal performance of roofs. An accurate estimation of the convective heat transfer coefficient is critical, since it is used to calculate the mass transfer coefficient, and thereby the condensation/evaporation related latent heat fluxes. Previous studies indicate that dew deposits could alter the apparent emissivity of roof surfaces significantly, especially low-emittance surfaces (e.g. metal-coated steel sheet roofs). However, it seems that previous studies into the effects of dew on roof thermal performance adopted convective heat transfer coefficient algorithms that were arguably not appropriate for roof-like surfaces, and did not consider changes in the apparent roof surface emissivity.

Analysis of the existing RP1037 experimental dataset revealed that condensation was likely to have formed on the roofs of all three buildings that were studied, on approximately 80% of the nights when monitoring took place. The spatially averaged roof surface temperature often decreased below the dew-point temperature by several degrees at night, and remained so for several hours. While these observations do not quantify the effects of dew on roof thermal performance, they do demonstrate how often dew can form in 'real-world' conditions. Furthermore, the frequent depression of roof surface temperatures several degrees below dew-point indicates that the latent heat released during the condensation process was insufficient to maintain the roof surface at or above the dew-point temperature.

A roof condensation model was formed, based on an energy balance surrounding the roof sheet and previously established sub-models for the various heat and mass fluxes that are involved. The model can track the formation and depletion of a water film on a roof surface, taking into account: i) the latent heat that is released during condensation and absorbed during evaporation, and ii) the effect of the water film on the effective thermal emittance of the roof top surface. Application of the model to several quasi-steady cases has revealed the effect of ambient air temperature and humidity on dew formation. During the remainder of this project, the roof condensation model will be applied to dynamic cases, to quantify the effect of dew condensation/evaporation on the performance of cool roofs, relative to low-emittance 'non-cool' roofs (e.g. metal-coated steel sheet roofs).

The above-roof temperature model, developed in RP1037, was further analysed, to determine the range of weather conditions and buildings for which it is valid. Even though the model was based on experiments conducted in relatively warm weather (near Sydney in summer and autumn), year-long BPS of cities in seven of the eight primary Australian climate zones did not involve many conditions for which the model is invalid. It was noted that the RP1037 experimental dataset, on which the model is based, does not include wind speeds greater than 10 m s^{-1}. However, this is unlikely to have had a significant effect on BPS results in RP1037, since: i) such high wind speeds were very infrequent in the cases simulated, and ii) the model has a diminished effect at high wind speeds, as the roof surface temperature is driven closer to the ambient air temperature by enhanced convective heat transfer, so near-roof air temperatures will also be closer to 'ambient'. Limitations in the types of buildings to which the above-roof temperature model should be applied, prior to any further validation, have also been quantified in this report.

Through the process of analysing the above-roof temperature model, an improvement on the previously reported (RP1037) fit to experimental data was found. Thus, a new, improved form of the model has been developed and presented in this report. The revision has reduced the RMS deviation between model predictions and the RP1037 near-roof air temperature measurements from 0.83°C to 0.56°C in unstable conditions (i.e. when the roof surface is hotter than the ambient air temperature).

Further work in this project, RP1037u1, will develop on the findings reported here, to quantify the effects of condensation and above-roof air temperatures on the value proposition of cool roofs.

References

Ambrose, D. and Karagiozis, A. (2007) 'Pressure Equalized Insulated Glass Units in Exterior Building Envelopes', *ASHRAE*.

ASHRAE (2009) *ASHRAE Handbook: Fundamentals*. Atlanta, GA, USA: American Society of Heating, Refrigeration and Air-Conditioning Engineers.

Australian Building Codes Board (2016) 'National Construction Code'. Available at: http://www.abcb.gov.au.

Bassett, M. R. and Trethowen, H. A. (1984) 'Effect of Condensation on Emittance of Reflective Insulation', *Journal of Thermal Insulation*. Sage PublicationsSage CA: Thousand Oaks, CA, 8(2), pp. 127–135. doi: 10.1177/109719638400800207.

Bergman, T. *et al.* (2011) *Fundamentals of heat and mass transfer*. 7th edn. Jefferson, USA: John Wiley & Sons.

Beysens, D. *et al.* (2005) 'Measurement and modelling of dew in island, coastal and alpine areas', *Atmospheric Research*. Elsevier, 73(1–2), pp. 1–22. doi: 10.1016/J.ATMOSRES.2004.05.003.

Beysens, D. *et al.* (2006) 'Application of passive radiative cooling for dew condensation', *Energy*. Pergamon, 31(13), pp. 2303–2315. doi: 10.1016/J.ENERGY.2006.01.006.

Blocken, B., Tominaga, Y. and Stathopoulos, T. (2013) 'CFD simulation of micro-scale pollutant dispersion in the built environment', *Building and Environment*, 64(0), pp. 225–230. doi: http://dx.doi.org/10.1016/j.buildenv.2013.01.001.

Bloudek, K. (1992) *Building physics II - 1. Calculation methods*, *CVUT Prague*.

Carter, G. (2011) 'Issues and solutions to more realistically simulate conventional and cool roofs', in *Proceedings of Building Simulation 2011: 12th Conference of international building performance simulation association (IBPSA). Sydney, 14–16 November 2011*.

Carter, G. and Kosasih, B. (2015) 'Not so cool roofs', in *AIRAH's Future of HVAC 2015 Conference*. Melbourne, Australia.

Castro, I. P. and Robins, A. G. (1977) 'The flow around a surface-mounted cube in uniform and turbulent streams', *Journal of Fluid Mechanics*. 04/11. Cambridge University Press, 79(2), pp. 307–335. doi: 10.1017/S0022112077000172.

Çengel, Y. A. and Boles, M. A. (2002) *Thermodynamics : an engineering approach*.

Clear, R. D., Gartland, L. and Winkelmann, F. C. (2003) 'An empirical correlation for the outside convective air-film coefficient for horizontal roofs', *Energy and Buildings*, 35(8), pp. 797–811. doi: https://doi.org/10.1016/S0378-7788(02)00240-2.

Costanzo, V. *et al.* (2014) 'Proper evaluation of the external convective heat transfer for the thermal analysis of cool roofs', *Energy and Buildings*, 77, pp. 467–477. doi: http://dx.doi.org/10.1016/j.enbuild.2014.03.064.

Downing, H. D. and Williams, D. (1975) 'Optical constants of water in the infrared', *Journal of Geophysical Research*. John Wiley & Sons, Ltd, 80(12), pp. 1656–1661. doi: 10.1029/JC080i012p01656.

Duffie, J. A. and Beckman, W. A. (2013) *Solar engineering of thermal processes*. 4th edn. New York, USA: John Wiley and Sons.

EnergyPlus (2010) 'EnergyPlus Engineering Reference: The Reference to EnergyPlus Calculations.' US Department of Energy.

Essah, E. A. *et al.* (2009) 'Condensation and moisture transport in cold roofs: effects of roof underlay', *Building Research & Information*. Routledge , 37(2), pp. 117–128. doi: 10.1080/09613210802645973.

Green, A. *et al.* (2018) *Driving Increased Utilisation of Cool Roofs on Large-Footprint Buildings*.

Hale, G. M. and Querry, M. R. (1973) 'Optical Constants of Water in the 200-nm to 200-μm Wavelength Region', *Applied Optics*. Optical Society of America, 12(3), p. 555. doi: 10.1364/AO.12.000555.

Holck, O. and Svendsen, S. (2004) 'Modeling of Microclimates', *Performance and Durability Assessment*. Elsevier, pp. 297–326. doi: 10.1016/B978-008044401-7/50023-7.

Hosseini, S. A., Kermani, A. M. and Arabhosseini, A. (2019) 'Experimental study of the dew formation effect on the performance of photovoltaic modules', *Renewable Energy*. Elsevier Ltd, 130, pp. 352–359. doi: 10.1016/j.renene.2018.06.063.

Ilse, K. *et al.* (2019) 'Dew as a Detrimental Influencing Factor for Soiling of PV Modules', *IEEE Journal of Photovoltaics*, 9(1), pp. 287–294. doi: 10.1109/JPHOTOV.2018.2882649.

Keller, J. (1985) 'Characterization of the Thermal Performance of Uncovered Solar Collectors by Parameters Including the Dependence on Wind Velocity', in *Workshop on solar assisted heat pumps with ground coupled storage, Vienna, Austria, 8 May 1985*. Available at: https://www.osti.gov/etdeweb/biblio/7837131 (Accessed: 21 February 2019).

Krauter, S. (2004) 'Increased electrical yield via water flow over the front of photovoltaic panels', *Solar Energy Materials and Solar Cells*. North-Holland, 82(1–2), pp. 131–137. doi: 10.1016/J.SOLMAT.2004.01.011.

Laboratory, L. B. (1994) *DOE2 engineers manual, Version 2.1A*. Los Alamos, NM.

Lee, S. W., Lim, C. H. and Salleh, E. @ I. Bin (2016) 'Reflective thermal insulation systems in building: A review on radiant barrier and reflective insulation', *Renewable and Sustainable Energy Reviews*.

Pergamon, 65, pp. 643–661. doi: 10.1016/J.RSER.2016.07.002.

Leonard, T. and Leonard, T. (2006) 'Stay Cool: A roof system on a Minnesota building demonstrates energy-saving technology', *Professional Roofing*. Available at: http://www.professionalroofing.net.

Maestre-Valero, J. F., Martin-Gorriz, B. and Martínez-Alvarez, V. (2015) 'Dew condensation on different natural and artificial passive surfaces in a semiarid climate', *Journal of Arid Environments*. Academic Press, 116, pp. 63–70. doi: 10.1016/J.JARIDENV.2015.02.002.

Mao, G. and Kurata, K. (1998) 'Changes in Porosity and Longwave Characteristics of Row Cover Non-woven Fabrics due to Condensation.', *Journal of Agricultural Meteorology*. The Society of Agricultural Meteorology of Japan, 54(2), pp. 161–165. doi: 10.2480/agrmet.54.161.

Martin, M. and Berdahl, P. (1984) 'Characteristics of infrared sky radiation in the United States', *Solar Energy*. Pergamon, 33(3–4), pp. 321–336. doi: 10.1016/0038-092X(84)90162-2.

Mcadams, W. H. (1942) *Heat transmission*. New York: McGraw-Hill.

Mirsadeghi, M. *et al.* (2013) 'Review of external convective heat transfer coefficient models in building energy simulation programs: Implementation and uncertainty', *Applied Thermal Engineering*, 56(1), pp. 134–151.

Mitchell, J. W. (1976) 'Heat transfer from spheres and other animal forms', *Biophysical Journal*. Cell Press, 16(6), pp. 561–569. doi: 10.1016/S0006-3495(76)85711-6.

Monteith, J. L. and Unsworth, M. H. (2013) *Principles of environmental physics*. 4th edn. London: Edward Arnold.

Paolini, R. *et al.* (2014) 'Effect of ageing on solar spectral reflectance of roofing membranes: Natural exposure in Roma and Milano and the impact on the energy needs of commercial buildings', *Energy and Buildings*, 84, pp. 333–343.

Pieters, J. G., Deltour, J. M. J. J. and Debruyckere, M. J. G. (1995) 'Onset of Condensation on the Inner and Outer Surface of Greenhouse Covers during Night', *Journal of Agricultural Engineering Research*. Academic Press, 61(3), pp. 165–171. doi: 10.1006/JAER.1995.1043.

Piscia, D. *et al.* (2012) 'A CFD greenhouse night-time condensation model', *Biosystems Engineering*. Academic Press, 111(2), pp. 141–154. doi: 10.1016/J.BIOSYSTEMSENG.2011.11.006.

Pisello, A. L., Santamouris, M. and Cotana, F. (2013) 'Active cool roof effect: impact of cool roofs on cooling system efficiency', *Advances in building energy research*, 7(2), pp. 209–221.

Richards, K. (2009) 'Adaptation of a leaf wetness model to estimate dewfall amount on a roof surface', *Agricultural and Forest Meteorology*, 149(8), pp. 1377–1383. doi: 10.1016/j.agrformet.2009.02.014.

Richards, P. J. *et al.* (2007) 'Wind-tunnel modelling of the Silsoe Cube', *Journal of Wind Engineering and Industrial Aerodynamics*, 95(9), pp. 1384–1399. doi: http://dx.doi.org/10.1016/j.jweia.2007.02.005.

Robinson, H. E., Cosgrove, L. A. and Powell, F. J. (1957) *Thermal resistance of airspaces and fibrous insulations bounded by reflective surfaces - Building Materials and Structures Report 151*.

Sidran, M. (1981) 'Broadband reflectance and emissivity of specular and rough water surfaces', *Applied Optics*. Optical Society of America, 20(18), p. 3176. doi: 10.1364/AO.20.003176.

Simpson, A., Castles, G. and O'Connor, D. E. (1992) 'Condensation, heat transfer and ventilation processes in flat timber-frame cold roofs', *Building Services Engineering Research and Technology*. Sage PublicationsSage CA: Thousand Oaks, CA, 13(3), pp. 133–145. doi: 10.1177/014362449201300302.

Sleiman, M. *et al.* (2011) 'Soiling of building envelope surfaces and its effect on solar reflectance—Part I: Analysis of roofing product databases', *Solar Energy Materials and Solar Cells*, 95(12), pp. 3385–3399.

Sleiman, M. *et al.* (2014) 'Soiling of building envelope surfaces and its effect on solar reflectance–Part II: Development of an accelerated aging method for roofing materials', *Solar Energy Materials and Solar Cells*, 122, pp. 271–281.

Tiwari, G. N., Kumar, A. and Sodha, M. S. (1982) 'A review—Cooling by water evaporation over roof', *Energy Conversion and Management*. Pergamon, 22(2), pp. 143–153. doi: 10.1016/0196-8904(82)90036-X.

Tywoniak, J. (1999) 'EFFECT OF LONGWAVE RADIATION IN COLD ROOFS-REMARKS ON SIMULATIONS', in *Proceedings of the International Building Performance Simulation Association*.

Walton, G. N. (1981) *Passive solar extension of the building loads analysis and system thermodynamics (BLAST) program*. Champaign, IL.

Wray, C. and Akbari, H. (2008) 'The effects of roof reflectance on air temperatures surrounding a rooftop condensing unit', *Energy and Buildings*, 40(1), pp. 11–28. doi: http://dx.doi.org/10.1016/j.enbuild.2007.01.005.

Xu, W. and Shen, S. C. (1992) 'Infrared radiation and reflection in an inhomogeneous coating layer on a substrate', *Applied Optics*. Optical Society of America, 31(22), p. 4488. doi: 10.1364/AO.31.004488.

ZOLOTAREV and VM (1969) 'Dispersion and Absorption of Liquid Water in Infrared and Radio Regions of Spectrum', *Opt Spectosc*, 26, pp. 430–432. Available at: https://ci.nii.ac.jp/naid/10020243930/ (Accessed: 27 February 2019).